

This discussion paper is/has been under review for the journal Earth System Science Data (ESSD). Please refer to the corresponding final paper in ESSD if available.

# Subglacial landforms beneath Rutford Ice Stream, Antarctica: detailed bed topography from ice-penetrating radar

E. C. King, H. D. Pritchard, and A. M. Smith

British Antarctic Survey, Cambridge, UK

Received: 15 October 2015 – Accepted: 26 October 2015 – Published: 12 November 2015

Correspondence to: E. C. King (ecki@bas.ac.uk)

Published by Copernicus Publications.

Subglacial landforms  
beneath Rutford Ice  
Stream, Antarctica

E. C. King et al.

Title Page

Abstract

Instruments

Data Provenance & Structure

Tables

Figures



Back

Close

Full Screen / Esc

Printer-friendly Version

Interactive Discussion



## Abstract

We present a digital elevation model of the bed of Rutford Ice Stream, Antarctica derived from radio-echo sounding data. The data cover an 18 km × 40 km area immediately upstream of the grounding line of the ice stream. This area is of particular interest because repeated seismic surveys have shown that rapid erosion and deposition of subglacial sediments has taken place. The bed topography shows a range of different subglacial landforms including mega-scale glacial lineations, drumlins and hummocks. This dataset will form a baseline survey which, when compared to future surveys, should reveal how active subglacial landscapes change over time. These data also allow comparison between subglacial landforms in an active system with those observed in deglaciated areas in both polar regions. The dataset comprises observed ice thickness data, an interpolated bed elevation grid, observed surface elevation data and a surface elevation grid. The dataset is available at <http://doi.org/269>.

## 1 Introduction

Subglacial bedforms develop where ice flows over a sedimentary substrate, but precisely how this happens is still the subject of much research (e.g. Clark, 2010; Menzies, 1989; Rose, 1987; Fowler, 2010). The size and shape of large numbers of palaeo landforms have been mapped from exposed former ice sheet beds by satellite, airborne and shipboard systems (e.g. Clark et al., 2009; Greenwood and Clark, 2010; Spagnolo et al., 2012) but accessing the bed of contemporary ice sheets for such studies is extremely difficult. While the basal topography beneath the Antarctic Ice Sheet is becoming better known at a spatial resolution of kilometres (Fretwell et al., 2013), there have been only a small number of surveys that provide spatial resolution of a few metres that are hence capable of showing the size and distribution of sub-glacial landforms (King et al., 2009, 2007).

<a href="#">Title Page</a>	
<a href="#">Abstract</a>	<a href="#">Instruments</a>
<a href="#">Data Provenance &amp; Structure</a>	
<a href="#">Tables</a>	<a href="#">Figures</a>
<a href="#">◀</a>	<a href="#">▶</a>
<a href="#">◀</a>	<a href="#">▶</a>
<a href="#">Back</a>	<a href="#">Close</a>
<a href="#">Full Screen / Esc</a>	
<a href="#">Printer-friendly Version</a>	
<a href="#">Interactive Discussion</a>	



Elongate landforms composed of till were first identified beneath Rutford Ice Stream using seismic surveying (Smith, 1997b; Smith and Murray, 2009). The dataset presented by King et al. (2009) used ice-penetrating radar to extend the mapping around the seismic lines to identify a suite of Mega-Scale Glacial Lineations (MSGs). This was 5 the first time MSGs were mapped beneath actively-flowing ice at a similar 3-D resolution to offshore swath bathymetry. That dataset was extended in the 2008–2009 Antarctic field season by further ground radar survey, covering an additional 25 km of the ice stream towards the grounding line. The combined dataset covers a 40 km × 18 km section of the bed, representing about 20 % of the fast-flowing part of the ice stream 10 (that portion flowing at more than  $100 \text{ m a}^{-1}$ ). In this paper, we present the combined dataset as a digital elevation model (DEM) of the bed which has grid dimensions of 100 m × 25 m. The DEM provides the opportunity to compare the metrics of landforms beneath an active ice stream with those from palaeo ice stream beds, it also sets the context for more detailed seismic and radar studies of Rutford Ice Stream. The DEM will 15 also act as a planning tool for bed-access drilling for sampling of substrate materials and measurement of basal conditions, as well as a baseline survey for the assessment of on-going erosion and deposition by repeat surveys in the future.

## 2 Location and previous work

The downstream portion of Rutford Ice Stream occupies a 26 km wide, 2.4 km deep 20 trough adjacent to the Ellsworth Mountains (Fig. 1). Repeated seismic reflection profiling (Smith, 1997a, 2007; Smith et al., 2007) showed that the bed of the ice stream is composed of a mixture of soft and stiff till; that the soft till was formed into elongate landforms; and that erosion and deposition of the basal sediment took place over short timescales. In one location an area 500 m across was eroded by 6 m in the 6 year 25 interval between seismic surveys (Smith, 1997a), over the following 7 years a mound of sediment 100 m across and 10 m high was emplaced in the same location. In addition,

[Title Page](#)

[Abstract](#)

[Instruments](#)

[Data Provenance & Structure](#)

[Tables](#)

[Figures](#)

◀

▶

◀

▶

[Back](#)

[Close](#)

[Full Screen / Esc](#)

[Printer-friendly Version](#)

[Interactive Discussion](#)



## Subglacial landforms beneath Rutford Ice Stream, Antarctica

E. C. King et al.

[Title Page](#)

[Abstract](#)

[Instruments](#)

[Data Provenance & Structure](#)

[Tables](#)

[Figures](#)

[◀](#)

[▶](#)

[◀](#)

[▶](#)

[Back](#)

[Close](#)

[Full Screen / Esc](#)

[Printer-friendly Version](#)

[Interactive Discussion](#)



the acoustic characteristics of sections of the till changed over the period indicating a transition from a soft, dilatant till to a stiff, lodged condition.

A radar survey of the bed topography surrounding the Smith (1997a, b) seismic lines, revealed a large suite of drumlins and mega-scale glacial lineations (MSGs) located in areas where the seismic surveys indicated soft, highly dilated, water-saturated sediment beneath the ice (King et al., 2009). Conversely, in areas where the seismic data indicated stiff till, the glacial landforms were much smaller, hummocky shapes. Over these hummocky areas, seismic recorders registered more micro earthquakes from the bed of the ice stream (indicative of stick-slip motion) than in areas where the soft, wet sediment was present (Smith, 2006), which were seismically “quiet” (thought to equate to a more continuous style of movement due to the greater lubrication of the bed). This was a further indication that basal resistance to flow can vary spatially on a small scale, potentially leading to a shifting pattern of lubricated and sticky spots within the bed of the ice stream.

The ice surface flow velocity over the area of the radar survey is  $365 \text{ m a}^{-1}$  at the upstream end, accelerating to  $400 \text{ m a}^{-1}$  at the grounding line (Gudmundsson, 2006). There is a modulation of the flow speed at the grounding line of up to 20 % with a fortnightly periodicity linked to the spring-neap tidal cycle (Gudmundsson, 2006). There was no significant variation in the flow speed of the ice stream over the 1979–2003 period (Gudmundsson and Jenkins, 2009).

### 3 Data acquisition, processing and visualisation

#### 3.1 Acquisition

The bed elevation data were derived from ground-based radar surveys. The radar data were collected over two field seasons using the British Antarctic Survey's Deep Look Radio Echo Sounder (DELORES), operating at 3 MHz (King et al., 2009). This is a monopulse radar operating in the 1–4 MHz range that is based on designs developed

**Subglacial landforms  
beneath Rutford Ice  
Stream, Antarctica**

E. C. King et al.

[Title Page](#)[Abstract](#)[Instruments](#)[Data Provenance & Structure](#)[Tables](#)[Figures](#)[|◀](#)[▶|](#)[◀](#)[▶](#)[Back](#)[Close](#)[Full Screen / Esc](#)[Printer-friendly Version](#)[Interactive Discussion](#)

by the University of Washington (Gades, 1998) and St Olaf College (Welch and Jacobel, 2003). The transmitter fires a  $\pm 2500$  V pulse into the antenna at a variable firing rate between 1 and 5 kHz. The antennae were resistively-loaded wire dipoles and the receiver used a chassis computer with a 100 MHz digitising card. The surveys reported

here were acquired using 20 m half-dipole antennas which results in a centre frequency of approximately 3 MHz. The transmitter was fired at a pulse repetition rate of 1 kHz and 1000 shots were stacked in the oscilloscope buffer to form each recorded trace in order to improve the signal to noise ratio. A trigger pulse was transmitted between transmitter and the receiving digitiser via a fibre-optic cable. The radar equipment was towed behind a snowmobile travelling at about  $12 \text{ km h}^{-1}$ , therefore each trace of the final record is built up of data acquired over a horizontal distance of circa 3 m.

Each survey took a two-person team about three weeks to acquire. Navigation along the pre-planned lines was done using single-frequency GPS units mounted on the snowmobiles. A dual-frequency GPS receiver was operated on the recording sledge to provide accurate post-hoc positions. Lines were oriented orthogonal to the ice flow, spaced 500 m apart. Some lines were acquired parallel to ice flow in order to check for any triggering discrepancies that could induce time shifts in the picked bed profiles.

### 3.2 Processing

The radar data were processed using ReflexW software (Sandmeier Scientific Software) in the following sequence:

- assign positioning information. The dual-frequency GPS data were processed using the kinematic-mode precise point positioning service provided by the Canadian Geodetic Service (<http://webapp.geod.nrcan.gc.ca/geod/tools-outils/ppp.php>). An offset was applied from the GPS antenna position (on the recording sledge) to the centre point of the antenna array to provide the geographic location of the reflection point on the bed.

- 5 – suppression of the effects of the direct (airwave + groundwave) arrival. The direct arrival is a very high amplitude pulse transmitted horizontally between the transmitting and receiving antennae. The effect on the receiving system is to induce wow in the amplifier, that is a high-amplitude, very low frequency overprint on the signal. Wow can be removed either by use of a frequency filter or by computing an average trace for the record and subtracting the average trace from each individual trace. The use of a bandpass filter on high amplitude signals can result in unwanted artefacts, particularly at the start and end of the record, so the average trace subtraction method was used here.
- 10 – bandpass filter. Frequencies below 0.5 MHz and above 10 MHz were suppressed to increase the signal-to-noise ratio.
- amplitude correction. The amplitudes were scaled proportional to the two-way travel time to compensate for the spherical spreading of the radar wave front.
- 15 – migration. The action of the migration step is to re-assign energy back to its source point, it has the effect of collapsing hyperbolae, correcting dipping events to true dip and improving horizontal resolution.

Figure 2a shows an example radar profile, displaying only that part of the record centred around the bed return. The display has high vertical exaggeration (7.5 : 1) to emphasise the shape of the landforms. The dominant event is the reflection from the bed of the ice stream. There is a very high degree of spatial correlation between each line (red lines in Fig. 2c).

20 The onset time of the bed reflection was determined at 7.5 m intervals along each line and converted to bed elevations with a precision of  $\pm 3$  m. The bed is an interface with a much higher reflection coefficient than any near-by internal ice layers so the precision of the radar range measurement is not affected by ambiguity in resolving the bed reflection from other reflections. The criteria that determine the precision of the range measurement are the rise time of the source signal; the bandwidth of the

[Title Page](#)[Abstract](#)[Instruments](#)[Data Provenance & Structure](#)[Tables](#)[Figures](#)[◀](#)[▶](#)[◀](#)[▶](#)[Back](#)[Close](#)[Full Screen / Esc](#)[Printer-friendly Version](#)[Interactive Discussion](#)

<a href="#">Title Page</a>
<a href="#">Abstract</a> <a href="#">Instruments</a>
<a href="#">Data Provenance &amp; Structure</a>
<a href="#">Tables</a> <a href="#">Figures</a>
<a href="#">◀</a> <a href="#">▶</a>
<a href="#">◀</a> <a href="#">▶</a>
<a href="#">Back</a> <a href="#">Close</a>
<a href="#">Full Screen / Esc</a>
<a href="#">Printer-friendly Version</a>
<a href="#">Interactive Discussion</a>

system; and the digitisation interval. Here we assume that there is no change in the wave speed profile between two adjacent measurements. In our system the output voltage rises at  $250 \text{ V ns}^{-1}$ , therefore the peak voltage is reached in 10 ns and the onset of the direct wave can be picked at the digital resolution which is 10 ns (i.e. the digitiser card samples the waveform at 10 ns intervals). The bandwidth of the recording system is 50 MHz with the result that reflections from high-contrast interfaces such as the bed have sharp onsets that can be easily picked for time of arrival. The remainder of the error budget for the bed elevation is made up of uncertainty in the GPS-derived elevation of the recording system and uncertainty in the depth-averaged wave velocity.

The horizontal resolution is a measure of the minimum size an object has to be to be distinguishable as a separate entity on the target of interest. The size of the Fresnel zone at quarter-wavelength is sometimes used as an estimate of horizontal resolution in radar data but that measure is only valid for unmigrated data. Migration collapses the size of the Fresnel zone to approximately one quarter of the dominant wavelength (Lindsey, 1989). Thus, the theoretical horizontal resolution of these migrated data is given by:

$$F_d = V_{\text{avg}}/4f \quad (1)$$

where  $F_d$  is the post-migration Fresnel diameter,  $V_{\text{avg}}$  is the average wave speed from surface to bed and  $f$  is the frequency. For  $V_{\text{avg}} = 0.167 \text{ m ns}^{-1}$  and the mean bandwidth frequency of 4.75 MHz,  $F_d = 8.8 \text{ m}$ , comparable with the horizontal trace spacing of 7.5 m.

The final step in the processing sequence was to convert the processed radar data to SEG-Y format to facilitate exchange of the data and import into interpretation software packages.

### 25 3.3 Picking the bed reflector and visualisation

The processed radar data files were imported into the Petrel<sup>TM</sup> Schlumberger interpretation software package. The times of the reflections from the bed of the ice stream



were picked on the radar profiles using a semi-automatic picker that followed the peak of the reflection wavelet from trace to trace. This created a raw dataset in  $x, y, t$  form where  $x$  and  $y$  were the coordinates in South Polar Stereographic projection and  $t$  was the two-way travel time. The measured point values were then interpolated onto

5 a 25 m (cross-flow)  $\times$  100 m (along-flow) grid oriented orthogonal to the profile lines using a natural neighbour algorithm with a 5 : 1 anisotropy ratio aligned along the ice flow direction (Fig. 2c). This interpolation scheme preserves the continuity of features elongate in the flow direction while preserving the high spatial sampling of the cross-flow bed profile.

10 The radar system determines the time-of-flight of the radio wave from the transmitter to the receiver via a reflection from the bed. This information was converted into elevation of the bed with respect to the WGS84 ellipsoid by using a time-to-depth conversion and then subtracting the depths from the surface elevation as recorded by the dual-frequency GPS system mounted on the recording sledge. The radar wave speed used for the time-to-depth conversion was  $0.167 \text{ m ns}^{-1}$ . The use of a single value of 15 radar wave speed for the depth conversion is a simplification, it does not take into account the variation in wave speed through the firn nor any variation with depth due to temperature, though these variations are likely to change slowly in the horizontal direction. We are not able to quantify these variations so the absolute elevations in the 20 WGS84 ellipsoid reference frame may be in error to the order of 10–20 m, even though the relative heights of the landforms are known to  $\pm 3 \text{ m}$ .

### 3.4 Results – map products

The bed elevation map is shown as Fig. 3, the same data, projected as a 3-D view, is shown in Fig. 4. On the large scale the bed has a W profile with troughs to either 25 side separated by a central ridge. The central ridge is subdued in the upstream portion of the survey area (labelled “Central Low Ridge” in Fig. 3) and much higher in the downstream portion (“Central High Ridge” in Fig. 3). There is a transition area between

<a href="#">Title Page</a>	
<a href="#">Abstract</a>	<a href="#">Instruments</a>
<a href="#">Data Provenance &amp; Structure</a>	
<a href="#">Tables</a>	<a href="#">Figures</a>
<a href="#">◀</a> <a href="#">▶</a>	
<a href="#">◀</a>	<a href="#">▶</a>
<a href="#">Back</a>	<a href="#">Close</a>
<a href="#">Full Screen / Esc</a>	
<a href="#">Printer-friendly Version</a>	
<a href="#">Interactive Discussion</a>	



## Subglacial landforms beneath Rutford Ice Stream, Antarctica

E. C. King et al.

[Title Page](#)

[Abstract](#)

[Instruments](#)

[Data Provenance & Structure](#)

[Tables](#)

[Figures](#)

[|◀](#)

[▶|](#)

[◀](#)

[▶](#)

[Back](#)

[Close](#)

[Full Screen / Esc](#)

[Printer-friendly Version](#)

[Interactive Discussion](#)



the low and high portions of the central ridge that resembles the “cow catcher” on an historic locomotive in 3-D view (Fig. 4).

In order to emphasise the smaller scale landscape features we computed a smoothed surface using a 2 by 2 km smoothing filter and subtracted this from the bed elevation surface. This has the effect of a high-pass spatial filter on the data. The 3-D surface in Fig. 4 is colour-coded with the residual elevation to make the individual landforms more clearly distinguishable.

The curvature of the bed surface is shown in map form in Fig. 5. This display emphasises the difference between highly-elongate linear features with sharply-defined profiles, elongate but subdued features and subdued features with low elongation ratios.

The surface elevation was derived from the dual-frequency GPS position information. Posted values at 7.5 m intervals along each survey line were used as input to create a surface model using convergent interpolation. The elevation in the upstream part of the survey is between 285 and 325 m above the WGS84 ellipsoid (Fig. 6), with no consistent downstream slope. A high point is reached near the centre of the survey which lies above the upstream end of the central ridge seen on the bed. The surface elevation downstream of this high point drops relatively steeply (by 70 m over 2 km) in the southeasterly direction.

There are several classes of subglacial bedform identified within the survey area (Fig. 7). A full description of the landforms will be presented elsewhere, here we summarise the main forms.

1. Parallel-sided MSGLs: The dominant features observed in the NE trough are parallel-sided MSGLs which have large elongation ratios and low amplitudes. These landforms are up to 17 km long and are spaced an average of 300 to 400 m apart (Spagnolo et al., 2014). In the NE trough, these features have a subtle kink in plan (Fig. 5), where they deviate toward the left margin of the ice stream in the region of the step in the bed. Parallel-sided MSGL in the SW trough are continuous for about 16 km and terminate downstream at a sharply-defined line.

5 2. Tapering drumlins: There are 6 features which lie within the field of MSGLs but which are distinctly different. These have higher trough-to-crest amplitudes (up to 70 m); a crest line that rises steeply to a maximum near the upstream end then tapers slowly downstream. Usually the troughs to either side reach their lowest points adjacent to the highest point on the crest.

10 3. Small drumlins or hummocks: the central and west-central parts of the survey are dominated by features with low amplitude and small elongation ratios (Fig. 7). In the south-western trough there is a small group of drumlins that have higher amplitudes and longer elongation ratios but are distinct from the MSGLs and separated from them by a distinct boundary.

15 4. Other linear features: The high region in the south central part of the survey has few positive streamlined features, the linear features that do exist are mostly grooves. On the west flank of the topographic high there is a step approximately 40 m high which is oriented at an angle to the ice flow.

## 15 4 Parameters for the gridded dataset

Details of the projection, limits and basic statistics of the data set are given in Table 1.

## 5 Limitations of the dataset

There is an implicit assumption in the acquisition and processing of single-source, single-receiver radar data that the reflection point lies vertically beneath the centre of the antenna array. This assumption is invalid under a number of circumstances, some of which can be corrected, others not. For reflection points that lie in the vertical plane through the profile line, reflections (or diffractions from point sources) can arise from points ahead of or behind the radar. Because the process of moving the system along

[Title Page](#)

[Abstract](#)

[Instruments](#)

[Data Provenance & Structure](#)

[Tables](#)

[Figures](#)

[◀](#)

[▶](#)

[◀](#)

[▶](#)

[Back](#)

[Close](#)

[Full Screen / Esc](#)

[Printer-friendly Version](#)

[Interactive Discussion](#)



the line renders these in-line but off-nadir reflections into hyperbolae on the record, they can be corrected during the migration processing step. However for reflection points lying off-nadir to either side of the line, it is not possible to reconstruct the original source point without additional cross-track records. Over large areas of the present survey this does not matter because the topography of the bed is largely two-dimensional and the line orientation was chosen to be orthogonal. The exceptions are areas where the bed slopes significantly in the in-flow direction, such as at the upstream or stoss end of drumlins, the upstream end of the Central High Ridge and the hummocky area in the centre of the survey. The effect is to limit the ability to accurately map the shape and position of the rounded ends of drumlins, even though the cross-profiles of the features is precisely known. We have conducted check surveys with closer cross-track spacing in some of the areas of potential uncertainty and find that the cross slopes are sufficiently shallow that side echoes do not map onto the in-line profile at times earlier than the vertical return from the bed.

The radar wave speed profile through the ice column is not known which means that values of ice thickness and therefore absolute bed elevation relative to sea level may have errors of circa 20 m. Radar waves travel through firn at a faster speed than through ice and at a slower speed through warm ice (i.e. ice near the pressure melting point) than through cold ice. We have few coincident seismic records that would provide an independent estimate of ice thickness, although these records are subject to similar uncertainties, so we have adopted a single value for the average wave speed. This uncertainty in the absolute elevation has no impact on the primary objective of the survey which was measurement and observation of subglacial landforms.

## 6 Significance

This dataset is the first to provide an extensive, high-resolution view of the landscape beneath an active ice stream. It will be of interest to those wishing to calibrate the palaeo record of ice stream tracks and to those seeking to understand the processes

[Title Page](#)[Abstract](#)[Instruments](#)[Data Provenance & Structure](#)[Tables](#)[Figures](#)[◀](#)[▶](#)[◀](#)[▶](#)[Back](#)[Close](#)[Full Screen / Esc](#)[Printer-friendly Version](#)[Interactive Discussion](#)

involved in generating subglacial landforms. All previous observations of fields of subglacial landforms have been from deglaciated regions, hence this dataset will enable the testing of theories concerning dewatering and sediment consolidation during the process of deglaciation. Given that repeat seismic surveys within the area have shown rapid rates of both erosion and deposition, this dataset forms a baseline survey for the assessment of sediment transport and landform evolution by way of repeat survey using similar techniques in the future. The dataset also allows the size and spatial distribution of landforms to be compared to the metrics of palaeo examples. The provision of the raw x, y, t picks in the dataset will facilitate precise re-survey and direct comparison of the raw data rather than the interpolated surfaces.

## Subglacial landforms beneath Rutford Ice Stream, Antarctica

E. C. King et al.

### Data availability

The dataset (King et al., 2015) can be accessed at <http://doi.org/269>.

**Acknowledgements.** We gratefully acknowledge the field assistants, pilots and operations staff of the British Antarctic Survey's Rothera Station for their support during the field data collection.

Schlumberger Plc is thanked for supplying educational licences for its Petrel software. This work was funded by BAS's Global Science in the Antarctic Context Programme (NERC award NE/B502287/1).

### References

- Clark, C. D.: Emergent drumlins and their clones: from till dilatancy to flow instabilities, *J. Glaciol.*, 56, 1011–1025, 2010.
- Clark, C. D., Hughes, A. L. C., Greenwood, S. L., Spagnolo, M., and Ng, F. S. L.: Size and shape characteristics of drumlins, derived from a large sample, and associated scaling laws, *Quaternary Sci. Rev.*, 28, 677–692, 2009.
- Fowler, A. C.: The formation of subglacial streams and mega-scale glacial lineations, *Proc. R. Soc. A-Math. Phys.*, 466, 3181–3201, 2010.

Fretwell, P., Pritchard, H. D., Vaughan, D. G., Bamber, J. L., Barrand, N. E., Bell, R., Bianchi, C., Bingham, R. G., Blankenship, D. D., Casassa, G., Catania, G., Callens, D., Conway, H., Cook, A. J., Corr, H. F. J., Damaske, D., Damm, V., Ferraccioli, F., Forsberg, R., Fujita, S., Gim, Y., Gogineni, P., Griggs, J. A., Hindmarsh, R. C. A., Holmlund, P., Holt, J. W., Jacobel, R. W., Jenkins, A., Jokat, W., Jordan, T., King, E. C., Kohler, J., Krabill, W., Riger-Kusk, M., Langley, K. A., Leitchenkov, G., Leuschen, C., Luyendyk, B. P., Matsuoka, K., Mouginot, J., Nitsche, F. O., Nogi, Y., Nost, O. A., Popov, S. V., Rignot, E., Rippin, D. M., Rivera, A., Roberts, J., Ross, N., Siegert, M. J., Smith, A. M., Steinhage, D., Studinger, M., Sun, B., Tinto, B. K., Welch, B. C., Wilson, D., Young, D. A., Xiangbin, C., and Zirizzotti, A.: Bedmap2: improved ice bed, surface and thickness datasets for Antarctica, *The Cryosphere*, 7, 375–393, doi:10.5194/tc-7-375-2013, 2013.

Gades, A. M.: Spatial and temporal variations of basal conditions beneath glaciers and ice sheets inferred from radio echo soundings, PhD, University of Washington, 1998.

Greenwood, S. L. and Clark, C. D.: The sensitivity of subglacial bedform size and distribution to substrate lithological control, *Sediment. Geol.*, 232, 130–144, 2010.

Gudmundsson, G. H.: Fortnightly variations in the flow velocity of Rutford Ice Stream, West Antarctica, *Nature*, 444, 1063–1064, 2006.

Gudmundsson, G. H. and Jenkins, A.: Ice-flow velocities on Rutford Ice Stream, West Antarctica, are stable over decadal timescales, *J. Glaciol.*, 55, 339–344, doi:10.3189/002214309788608697, 2009.

King, E. C., Hindmarsh, R. C. A., and Stokes, C. R.: Formation of mega-scale glacial lineations observed beneath a West Antarctic ice stream, *Nat. Geosci.*, 2, 585–588, 2009.

King, E. C., Pritchard, H. D., and Smith, A. M.: Rutford Ice Stream bed elevation DEM from radar data, In Centre, P. D., ed., Cambridge, U. K., 2015.

King, E. C., Woodward, J., and Smith, A. M.: Seismic and radar observations of subglacial bed forms beneath the onset zone of Rutford Ice Stream Antarctica. *J. Glaciol.*, 53, 665–672, 2007.

Lindsey, J. P.: The Fresnel zone and its interpretive significance, *The Leading Edge*, 8, 33–39, 1989.

Menzies, J.: Drumlins – Products of Controlled or Uncontrolled Glaciodynamic Response, *Quaternary Sci. Rev.*, 8, 151–158, 1989.

Rose, J.: Drumlins as part of a glacier bedform continuum, in: *Drumlin Symposium*, edited by: Menzies, J. and Rose, J., Rotterdam, Balkema, 360, 1987.

## Subglacial landforms beneath Rutford Ice Stream, Antarctica

E. C. King et al.

[Title Page](#)

[Abstract](#)

[Instruments](#)

[Data Provenance & Structure](#)

[Tables](#)

[Figures](#)

◀

▶

◀

▶

[Back](#)

[Close](#)

[Full Screen / Esc](#)

[Printer-friendly Version](#)

[Interactive Discussion](#)



**Subglacial landforms  
beneath Rutford Ice  
Stream, Antarctica**

E. C. King et al.

- Smith, A. M.: Basal conditions on Rutford Ice Stream, West Antarctica, from seismic observations, *J. Geophys. Res.-Sol. Ea.*, 102, 543–552, 1997a.
- Smith, A. M.: Variations in basal conditions on Rutford ice stream, west Antarctica. *J. Glaciol.*, 43, 245–255, 1997b.
- 5 Smith, A. M.: Microearthquakes and subglacial conditions, *Geophys. Res. Lett.*, 33, L24501, doi:10.1029/2006GL028207, 2006.
- Smith, A. M.: Subglacial bed properties from normal-incidence seismic reflection data, *J. Environ. Eng. Geoph.*, 12, 3–13, 2007.
- 10 Smith, A. M. and Murray, T.: Bedform topography and basal conditions beneath a fast-flowing West Antarctic ice stream, *Quaternary Sci. Rev.*, 28, 584–596, doi:10.1016/j.quascirev.2008.05.010, 2009.
- Smith, A. M., Murray, T., Nicholls, K. W., Makinson, K., Aoalgeirsdottir, G., Behar, A. E. and Vaughan, D. G.: Rapid erosion, drumlin formation, and changing hydrology beneath an Antarctic ice stream, *Geology*, 35, 127–130, 2007.
- 15 Spagnolo, M., Clark, C. D., and Hughes, A. L. C.: Drumlin relief, *Geomorphology*, 153, 179–191, 2012.
- Welch, B. C. and Jacobel, R. W.: Analysis of deep-penetrating radar surveys of West Antarctica, US-ITASE 2001, *Geophys. Res. Lett.*, 30, 1444, doi:10.1029/2003GL017210, 2003.

Discussion Paper | Discussion Paper

[Title Page](#)[Abstract](#)[Instruments](#)[Data Provenance & Structure](#)[Tables](#)[Figures](#)[|◀](#)[▶|](#)[◀](#)[▶](#)[Back](#)[Close](#)[Full Screen / Esc](#)[Printer-friendly Version](#)[Interactive Discussion](#)

## Subglacial landforms beneath Rutford Ice Stream, Antarctica

E. C. King et al.

[Title Page](#)

[Abstract](#)

[Instruments](#)

[Data Provenance & Structure](#)

[Tables](#)

[Figures](#)

◀

▶

◀

▶

[Back](#)

[Close](#)

[Full Screen / Esc](#)

[Printer-friendly Version](#)

[Interactive Discussion](#)



**Table 1.** Projection: Antarctic Polar Stereographic, WGS84 ellipsoid, Prime Meridian 0.0, Standard Parallel 71° S.

Axis	Min	Max
X	-1 299 211.26	-1 258 669.79
Y	124 167.22	154 725.41
Depth [m] (below WGS84 ellipsoid)	-2185.76	-1476.94
Lat	78°23'51.3927" S	78°00'1.0350" S
Long	84°32'26.7107" W	82°59'30.9101" W
Increment in X direction:	100	
Increment in Y direction:	25	
Unrotated Xmin:	-1 293 677.31	
Unrotated Ymin:	124 167.22	
Unrotated Xmax:	-1 254 477.31	
Unrotated Ymax:	143 242.22	
Rotation angle:	18.6	
Number of 2-D nodes in I direction:	393	
Number of 2-D nodes in J direction:	764	
<b>Topography Statistics</b>		
Min:	-2185.76	m
Max:	-1476.94	m
Delta:	708.82	m
Number of defined values:	244 280	
Mean:	-1858.71	m

**Subglacial landforms  
beneath Rutford Ice  
Stream, Antarctica**

E. C. King et al.

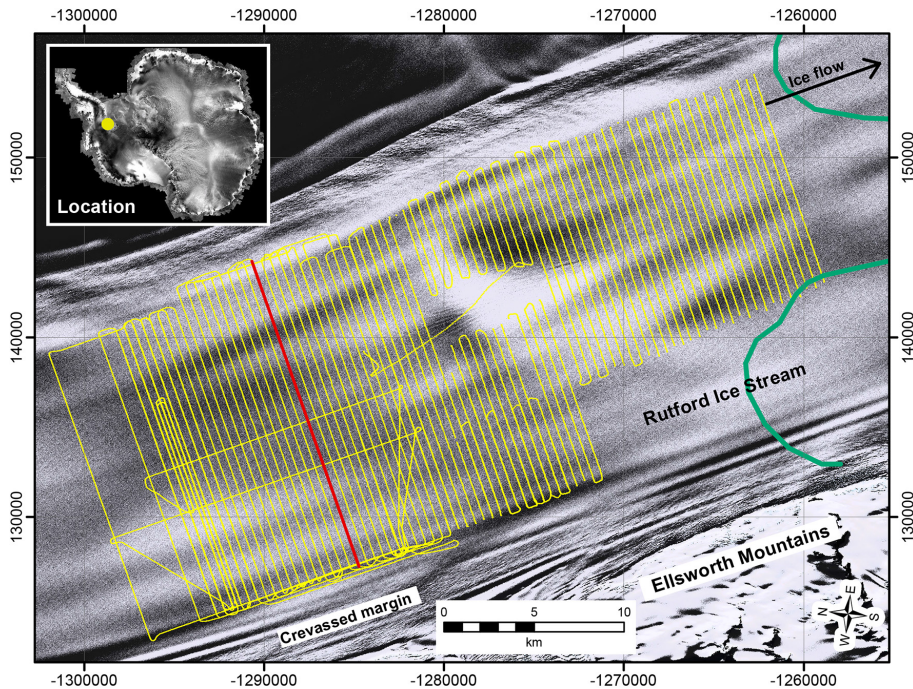


**Figure 1.** Location map. Rutford Ice Stream flows towards the south east past the Ellsworth Mountains at between  $365$  and  $400\text{ m a}^{-1}$ . Radar survey lines shown in yellow. Lines are spaced  $500\text{ m}$  apart. Gaps in the coverage are due either to equipment failure or the need to avoid crevasses. The grounding line is shown in green. Location of profile line shown in Fig. 2 marked in red. Polar Stereographic Projection. Axes are meters from South Pole.

[Title Page](#)[Abstract](#)[Instruments](#)[Data Provenance & Structure](#)[Tables](#)[Figures](#)[|◀](#)[▶|](#)[◀](#)[▶](#)[Back](#)[Close](#)[Full Screen / Esc](#)[Printer-friendly Version](#)[Interactive Discussion](#)

**Figure 2.** Detail of radar data. **(a)** Portion of radar profile across Rutford Ice Stream, windowed around the ice/sediment interface. **(b)** Close-up of interface reflection. The reflection is a negative-positive-negative wavelet (white-black-white on the grey-scale record) with a very high signal-to-noise ratio which allows very precise determination of the travel time. **(c)** 3-D view of the data (red lines) and interpolated grid (black lines) which shows the coherence of the picked data from line to line and shows that the gridded data faithfully reproduce the observed data.

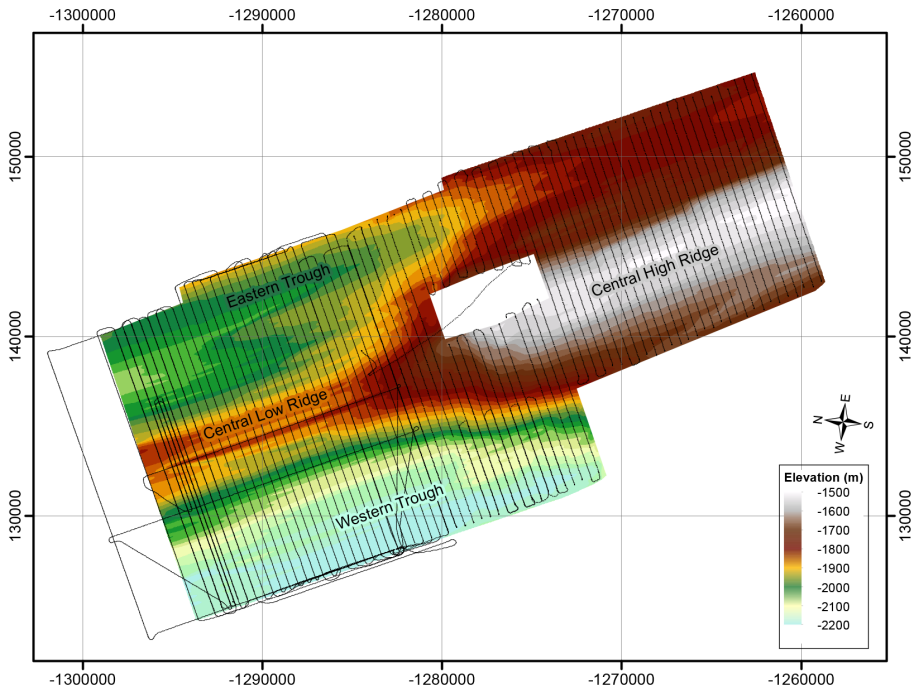


**Figure 3.** Map of bed elevation, referenced to the WGS84 ellipsoid. The difference between the ellipsoid and mean sea level is not known in this region. The bed of the ice stream has a W profile with a central ridge and troughs to either side. The downstream portion of the central ridge is several hundred meters higher than the surroundings and is likely to be a bedrock outcrop. Labels refer to features described in the text.

**Subglacial landforms  
beneath Rutford Ice  
Stream, Antarctica**

E. C. King et al.

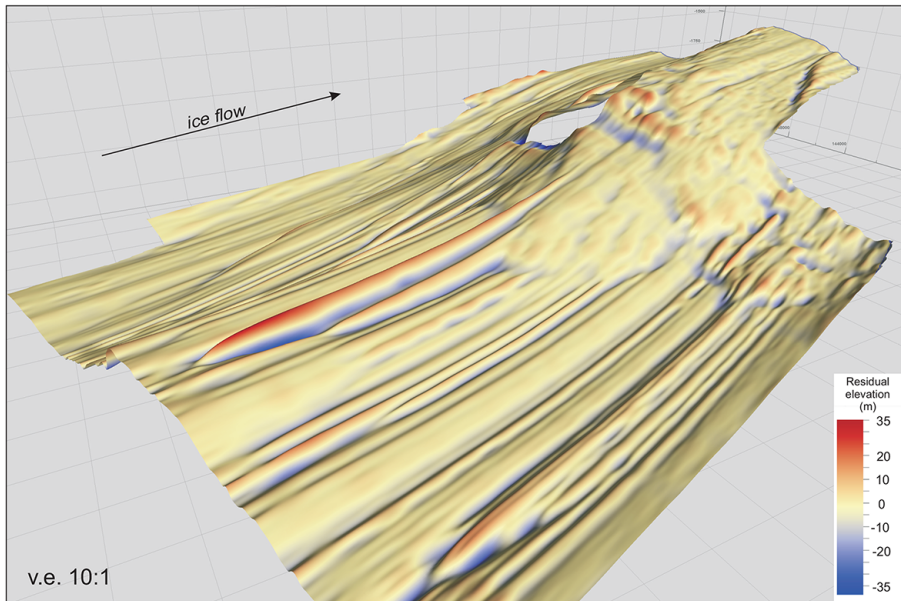


**Figure 4.** 3-D view of the gridded dataset. View is downstream towards the south east, vertical exaggeration is approximately 10 to 1. The bed elevation surface has been colour-coded by residual elevation to emphasise the landforms. Residual elevation was computed by differencing the bed elevation surface with a smoothed version which used a  $2\text{ km} \times 2\text{ km}$  spatial smoothing filter.

[Title Page](#)[Abstract](#)[Instruments](#)[Data Provenance & Structure](#)[Tables](#)[Figures](#)[|◀](#)[▶|](#)[◀](#)[▶](#)[Back](#)[Close](#)[Full Screen / Esc](#)[Printer-friendly Version](#)[Interactive Discussion](#)

**Subglacial landforms  
beneath Rutford Ice  
Stream, Antarctica**

E. C. King et al.

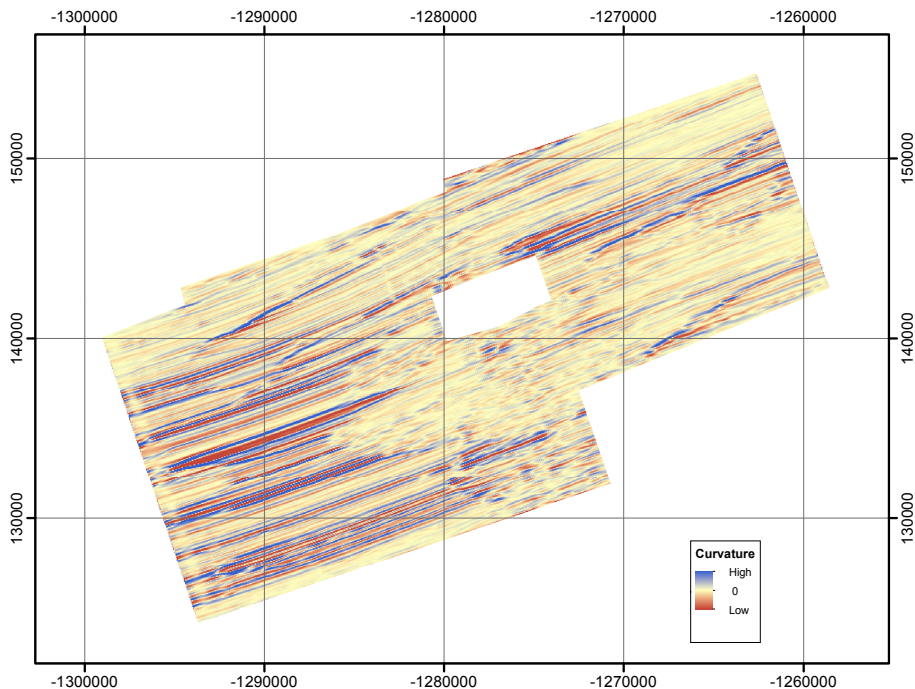


**Figure 5.** Map of the curvature of the bed elevation surface. This method of presenting the data emphasises the contrasts between high amplitude linear features, low amplitude linear features and low amplitude features with low elongation.

Discussion Paper | Discussion Paper

Discussion Paper | Discussion Paper

Discussion Paper | Discussion Paper

[Title Page](#)[Abstract](#)[Instruments](#)[Data Provenance & Structure](#)[Tables](#)[Figures](#)[◀](#)[▶](#)[◀](#)[▶](#)[Back](#)[Close](#)[Full Screen / Esc](#)[Printer-friendly Version](#)[Interactive Discussion](#)

**Figure 6.** Map of the elevation of the surface of the ice stream referenced to the WGS84 ellipsoid. Data was collected using a dual-frequency GPS unit on the radar receiver sledge and post-processed using a kinematic technique (see text). Steepest surface slope occurs above the upstream end of the bedrock outcrop that forms the central high ridge at the bed.

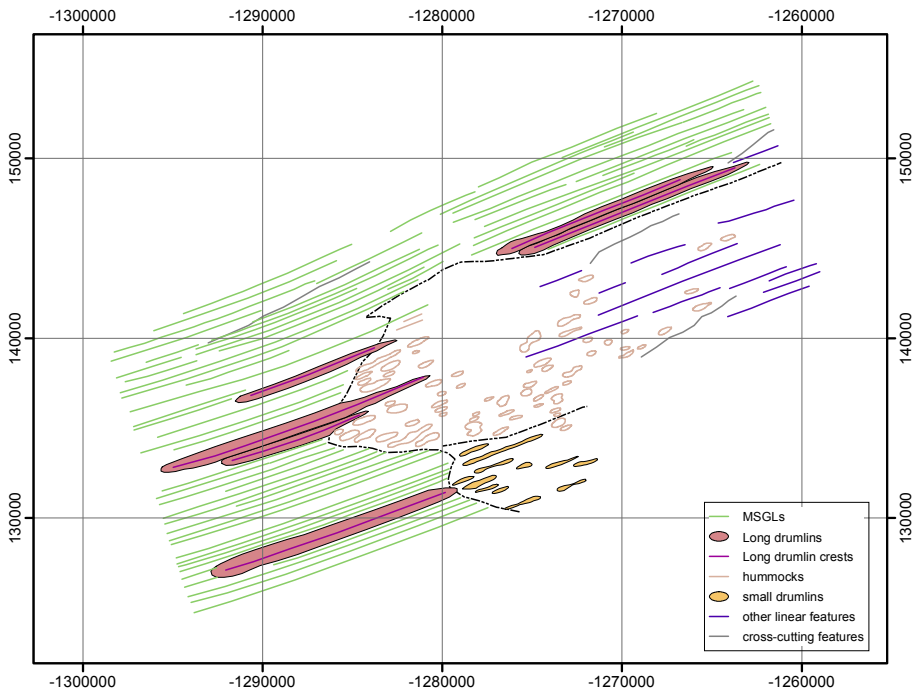


**Figure 7.** Geomorphological interpretation. The features of the bed of the ice stream can be classified into a number of different landforms and surface features, based on amplitude, length, outline shape and whether they are positive or negative landscape elements. See text for full descriptions of each class.